A PASSIVE HORN STRUCTURE WITH TRANSITIONS TO MICROSTRIP FOR QUASI-OPTICAL AMPLIFIER ARRAYS

Carlos E. Saavedra, Warren Wright, and Richard C. Compton[†]

Cornell University, School of Electrical Engineering
Phillips Hall, Ithaca, New York 14853
[†]*Lucent Technologies, 890 Tasman Dr., Milpitas, CA 95035-7912*

ABSTRACT

AN inclined-plane dual-horn structure is presented that couples energy from free-space to microstrip and back to free-space again. The structure consists of two back-to-back inclined planes that taper down to a common parallel-plate waveguide. The energy is fed from the parallel-plate waveguide to the microstrip using a transition that also serves as a power splitting network. The insertion loss from free-space to microstrip for the passive array is better than -2.5 dB from 30 to 47.5 GHz .

II. INTRODUCTION

ONE of the critical issues in spatial, or quasi-optical, power combining arrays is the *efficient* coupling of energy from free-space to the printed circuit transmission lines that feed the active elements. To couple the energy from free-space, numerous designs[1-5] have used arrays of planar antennas, with each antenna usually connected or coupled to one or two active elements. The drawback of using planar antennas is that the antennas are inefficient because a noticeable fraction of the energy fed to them is not radiated but is coupled to substrate modes[6,7]. Furthermore, with the exception of log-periodic and endfire antennas, printed antennas tend to be narrowband[6-8], consequently the arrays typically only have about a 5% bandwidth. Finally, the large amount of area occupied by the printed antennas leaves little room on the substrates for using multi-stage amplifiers in the arrays, thus limiting the output power capabilities of the arrays.

In this paper, a spatial power combiner is presented that overcomes some of the shortcomings of the printed antenna arrays by using a novel dual-horn antenna structure (Figure 1). The proposed array can power-combine a large number of active elements but it only uses one input and one output antenna, thus yielding good power-combining efficiencies. In addition, the design is broadband and the free-space to microstrip insertion loss is below -2.5 dB . Furthermore, multi-stage amplifiers can be cascaded as there are no restrictions on the longitudinal dimension of the array. The array in Figure 1 is 'one-dimensional' because it can house $1 \times n$ active elements. The number of active

Part of the 4th International Conference on Millimeter and Submillimeter Waves and Applications • San Diego • July 1998
SPIE Vol. 3465 • 0277-786X/98/$10.00

elements used can be substantially increased by making an $n \times n$ array by using the tapered grating array[9,10] depicted in Figure 2. The passive and active circuitry is identical for both arrays, but the array in Figure 2 uses a tapered grating to couple the energy from free-space. The tapered grating concept pre-dated the dual-horn concept. The dual-horn array was initially conceived to serve as a testbed for the microstrip circuits before incorporating them in the two-dimensional array.

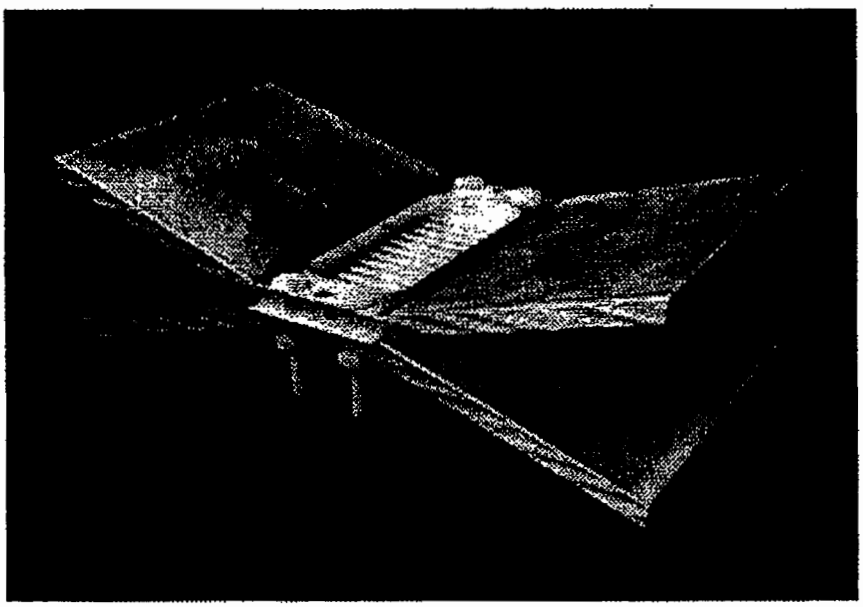

(a)

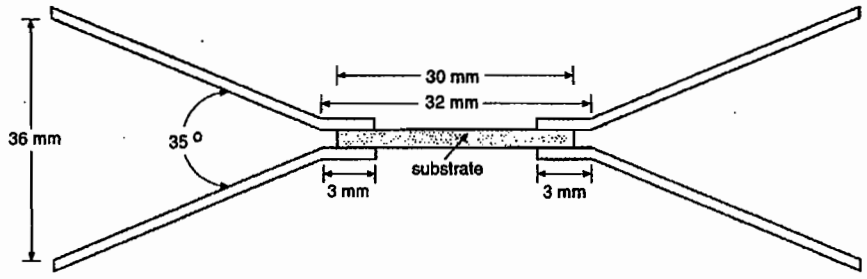

(b)

Figure 1Passive dual-horn structure. (a) Photograph of the passive array and (b) cross-sectional view. The microstrip circuitry is stacked between the two plates of the structure.

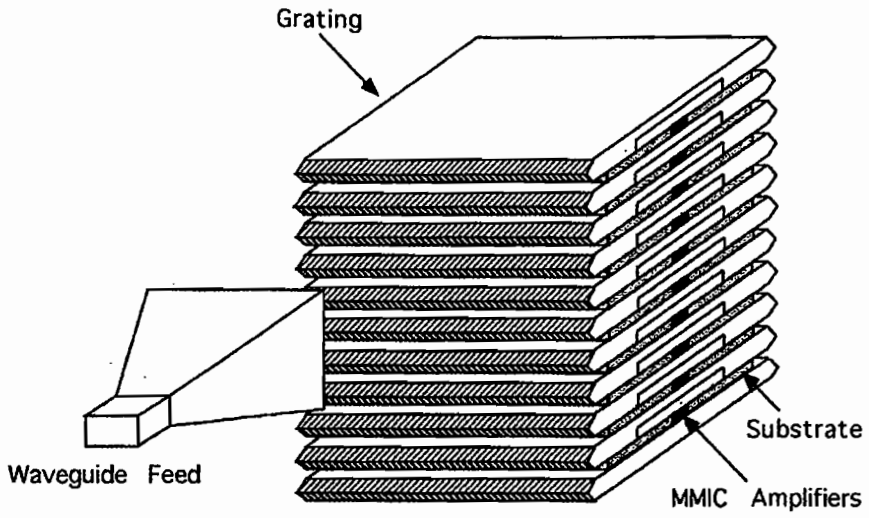

Figure 2 Millimeter-Wave Tapered Grating Amplifier Array. The amplifiers are approximately spaced $\lambda/2$ apart in both the horizontal and vertical dimension at the operating frequency. Lenses (not shown) are used to focus the beam from the waveguide feed to the grating.

Section III of this paper will document in detail the design of the dual-horn passive array. In section IV the Gaussian beam test setup used to measure the array will be discussed. Section V will be devoted to the measurement results, and finally Section VI will conclude the work.

III. DUAL-HORN ARRAY DESIGN

REFERRING to Figure 1b, energy is incident on the dual-horn structure from the left and it travels down the inclined-plane waveguide until it reaches the parallel-plate waveguide region. Stacked between the parallel plates is the microwave substrate with the waveguide to microstrip transitions, which also serve as a power splitting network. The energy then propagates through ten microstrip lines and it is recombined using a power combiner identical to the power splitting network. The energy is radiated to free-space by using another inclined-plane waveguide horn.

The flare angle of the horn antennas is 35°, a value that was selected after testing antennas with various linear and exponential flares. The height of the horn aperture was 36 mm , the aperture width was 75 mm , and the slant height was 57.2 mm . As shown in Figure 1b, a small sectio of air filled parallel-plate waveguide exists at both sides betweent the throat of the horn and the beginning of the dielectric filled waveguide region. That segment of air-filled waveguide, typically about 1 mm , works as an impedance mathching element between the horn impedance and the impedance of the dielectric-filled waveguide.

The substrate material used for the microstrip circuitry was 15-mil (0.381 mm) thick TMM3 from the Rogers Corporation with 0.5 oz. copper cladding on both sides. The TMM3 substrate is rigid and it has a nominal dielectric constant of 3.27.

Figure 3a shows a schematic diagram of the microstrip transitions. In the design process it was assumed that there was an infinite array of transitions (a reasonable assumption for the center elements of the array). The periodicity of the fields in the structure allows magnetic walls to be inserted in the array as shown in Figure 3b. The microstrip transitions were designed by considering only one transition section.

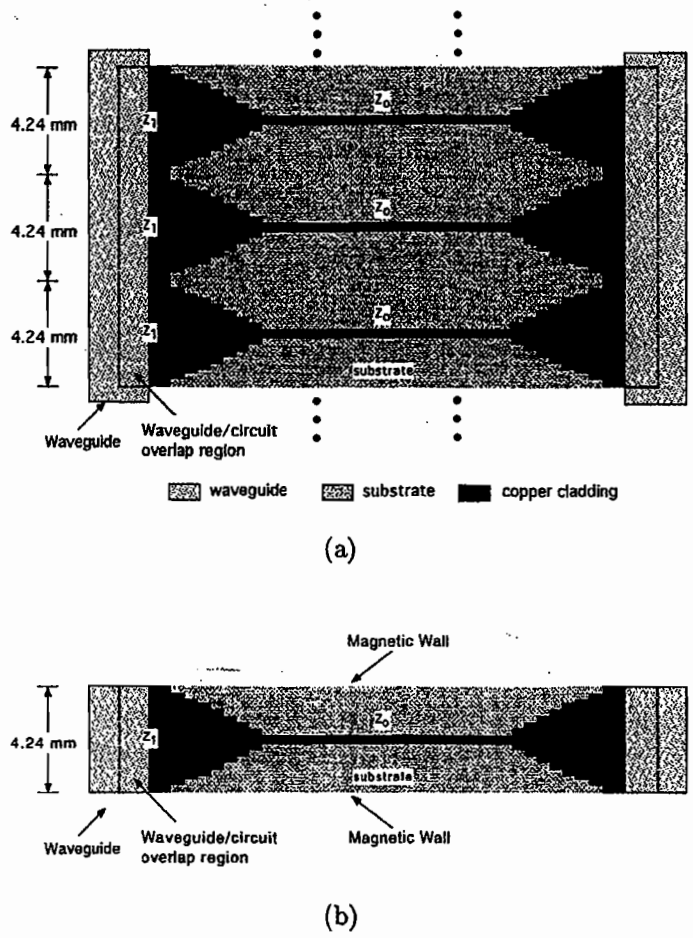

Figure 3 Parallel-plate waveguide to microstrip transitions. The periodicity of the array in (a) allows the use of magnetic walls to simplify the circuit to just one transition (b).

The width of each transition was 4.24 mm . Impedance Z_1 in Figure 3b is given by $Z_1 = \eta_o d/(w\sqrt{\epsilon_r})$. Using $d = 0.381$ mm , $w = 4.24$ mm , and $\epsilon_r = 3.27$ gives $Z_1 = 18.7\Omega$. The impedance from the overlap region in Figure 3b to the beginning of the

microstrip transmission lines is also Z_1. The final step in the transition design is to create a broadband matching network from Z_1 to Z_0, the impedance of the microstrip line that feeds the amplifier elements. The task was accomplished using seven $\lambda/4$ microstrip lines at the design frequency of 44 GHz.

The amplifiers used in the array discussed in Ref. 10 had 50Ω input and output impedance lines on the chip. The size of the bondpads on the MMIC was 100μm by 100μm, which was large enough for one or at most two bondwires from the MMIC to the microstrip lines on the TMM3 substrate. The first microstrip transitions used $Z_0 = 50\Omega$ but it was quickly discovered that because the transmission lines were 900μm wide and the bondwires were 31.75μm in diameter, the large step discontinuity between the two lines was causing large reflections in the signal. Although using a material with a higher dielectric constant would have made the 50Ω lines narrower, it was determined that the losses were greater when high ϵ_r substrates were used at Q-Band. The solution to the problem was to use higher impedance transmission lines. A transmission line width of 400μm was selected and the corresponding impedance was $Z_0 = 79.3\Omega$ for the substrate with $\epsilon_r = 3.27$.

IV. MEASUREMENT SYSTEM

A focused Gaussian beam test measurement system[9,11] was used to measure the s-parameters of the dual-horn array. Ka-Band pyramidal horns were used to launch and receive the Gaussian beam and lenses with focal lengths of 85 mm and 150 mm were used to focus the beam to the device under test (DUT). Since the measurement range was from 25 to 50 GHz, the positions of the lenses were calculated[12] so that the beam was focused on the DUT at 37.5 GHz .

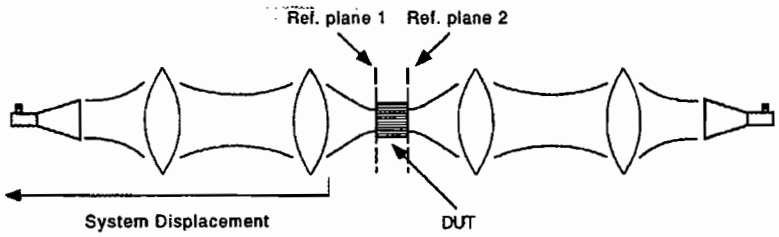

Figure 4 Gaussian beam measurement system. The reference planes were split by physically moving the left half of the setup as shown.

To perform two-port measurements on the dual horn structure, a full two-port calibration procedure for the Gaussian beam test setup was used. The calibration standards used were a zero length thru, a short, an offset short, and a load. After calibration the

reference planes were at the middle of the optical setup. Because the DUT is many wavelengths long in the direction of propagation, a way had to be found to place the reference planes at the input and output of the microstrip circuits. Since the excitation signals are Gaussian beams and their field intensity changes as a function of distance, it was not possible to simply to use an electrical delay[13] on the network analyzer to receede the reference planes. The solution was to mount the left-half of the setup on a movable stage, as suggested in Figure 4. After the calibration procedure, the stage was moved the desired distance and the reference planes were thus split. For the dual-horn antenna measurements, the reference planes were split by 32 mm, placing the reference planes at the throats of the horns[10].

V. EXPERIMENTAL RESULTS

FIGURE 5 shows the gated s-parameter measurements of the dual horn structure with the waveguide to microstrip transitions. The results reveal that the insertion loss from the input horn to the output horn is between -3 dB and -5 dB from 30 GHz to 47.5 GHz. Therefore, the insertion loss from free-space to microstrip is better than -2.5 dB in that frequency range, implying a 17.5 GHz bandwidth.

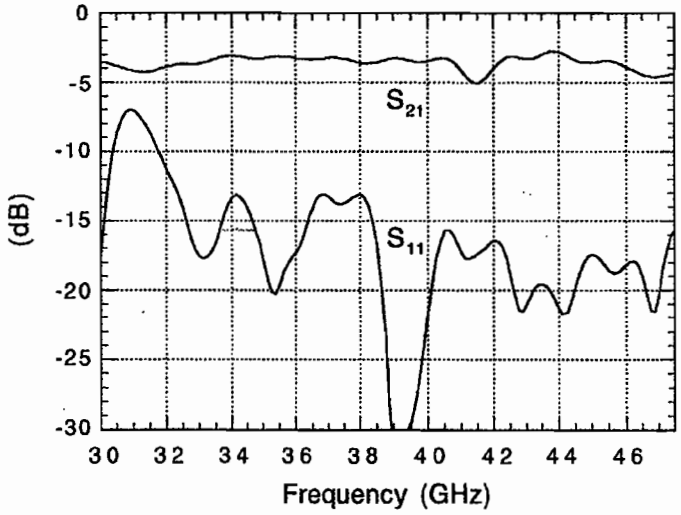

Figure 5 Dual horn antenna measurements with parallel-plate waveguide to microstrip transitions.

To investigate what happened to a Gaussian beam as it passed through the passive dual-horn structure, far-field measurements were made using a beam scanning system.

The lenses and receiving horn antenna on the right-half of the setup shown in Figure 4 were removed and the beam scanner was placed at $80\lambda_0$ from the DUT. In Figure 6, the magnitude of the electric field is plotted. There is bright central spot which strongly suggests that the Guassian beam has preserved its TEM_{00} mode. Side lobes are also observed on the plot, and it is believed that they arise from the rectangular aperture of the launching horn antenna on the far left of the test setup (Figure 4). Since only ~87% of the energy launched from that horn is coupled to the fundamental Gaussian mode, the rest of the energy is coupled into higher order modes.

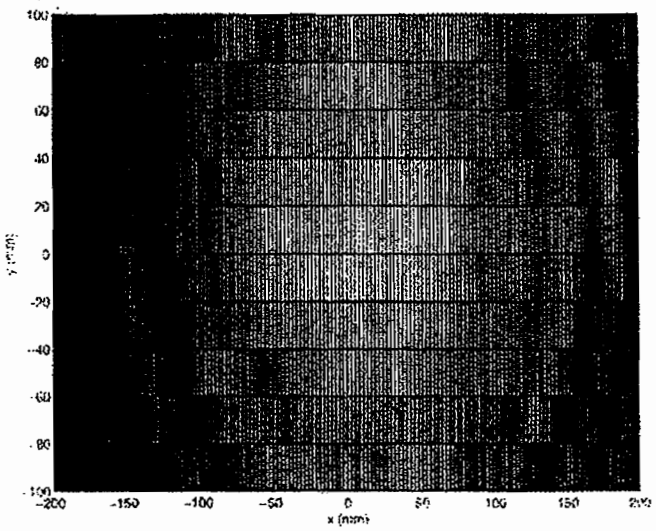

Figure 6 Passive dual-horn structure far-field plot of the electric field. The measurement was made at $80\lambda_0$ from the structure.

To improve the transmission loss, an anti-reflection, or 'moth-eye,' surface[14,15] was tested on the substrate board (Figure 7). The concept was to reduce the reflection caused at the abrupt air-dielectric interface in the parallel-plate waveguide by creating a gradual dielectric transition. The period of the the saw-teeth in Figure 7b is 2.0 mm and their depth is 1.75 mm.

Figure 8 compares the performance of the moth-eye board with the straight-edge board. An improvement of 0.6 dB is observed in S_{21} from 25 to 41 GHz using the board with the moth-eye edges. However, from 43 to 44.5 GHz, the serrated board performed worse than the straight-edge board. Studies with 2-D anti-reflection surfaces[15] suggest that best results are obtained with trench depths greater than $\lambda/2$. With an operating frequency of 44 GHz, the trench depth would need to be 3.4 mm instead of 1.75 mm, requiring the substrate boards to have an extra 3.3 mm in length, making themm too long to fit in the dual-horn structure.

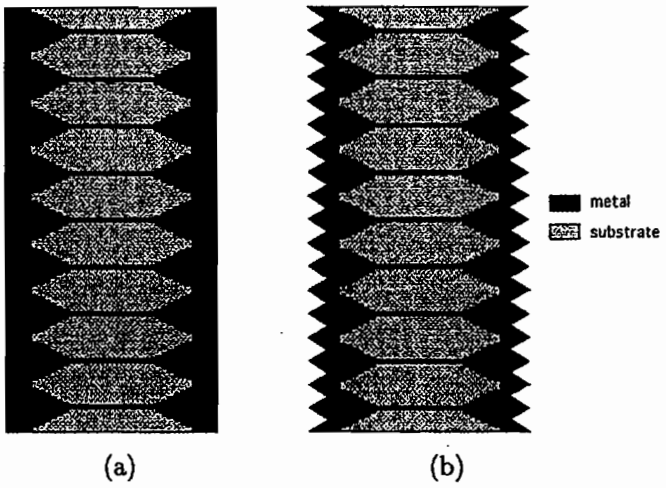

Figure 7 Microstrip transitions (a) board with straight edges, and (b) board with anti-reflection or moth-eye edges. The period of the sawteeth is 2.0 mm and their depth is 1.75 mm.

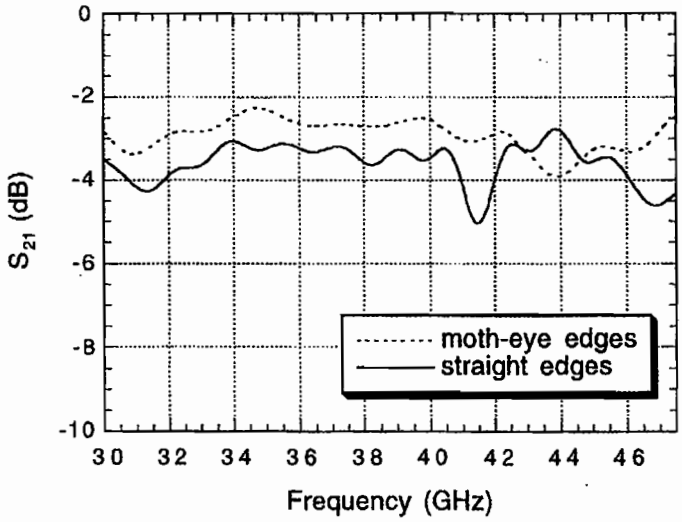

Figure 8 Comparison of transmission loss measurements of substrate boards with moth-eye edges and straight edges.

VI. CONCLUSION

A new structure for spatial power combining has been presented. The insertion loss of the passive structure is between -3 dB and -5 dB over a 17.5 GHz span. An active version[10] of the passive array has already been demonstrated and it has an average gain of 7 dB and a 3-dB bandwidth of 5.75 GHz .

VII. REFERENCES

1. R. A. York and Z. B. Popović, Eds., *Active and Quasi-Optical Arrays for Solid-State Power Combining,* New York: Wiley 1997.

2. T. Ivanov and A. Mortazawi, "Quasi-Optical Microstrip Amplifiers Based on Multi-layer Coupled Structures," *IEEE MTT-S Digest,* pp. 99-102, 1995.

3. T. Ivanov and A. Mortazawi, "A Two-Stage Spatial Amplifier with Hard Horn Feeds," *IEEE Microwave and Guided Wave Lett.*, Vol. 6, No. 2, pp. 88-90, 1996.

4. M. A. Gouker, J. T. Delisle, and S. M. Duffy, "A 16-element Subarray for Hybrid-Circuit Tile-Approach Spatial Power Combining," *IEEE Trans. Microwave Theory Tech.*, Vol. 44, No. 11, pp. 2093-2098, 1996.

5. C. W. Pobanz, J. Lin, and T. Itoh, "Active Integrated Antennas for Microwave Wireless Systems," *International Symposium on Signals, Systems, and Electronics,* pp. 1-4, Oct. 1995.

6. N. G. Alexopoulos, P. B. Katehi, and D. B. Rutledge, "Substrate Optimization for Integrated Circuit Antennas," *IEEE Trans. Microwave Theory Tech.*, Vol. MTT-31, No. 7, pp. 550-557, 1983.

7. D. M. Pozar, "Considerations for Millimeter Wave Printed Antennas," *IEEE Trans. Antennas and Propagat.*, Vol. AP-31, No. 5, pp. 740-747, 1983.

8. K. R. Carver and J. W. Mink, "Microstrip Antenna Technology," *IEEE Trans. Antennas and Propagat.*, Vol. AP-29, No. 1, pp. 2-24, 1981.

9. C. E. Saavedra, *An Integrated Millimeter-Wave Power Combiner using Three-Dimensional Tapered Gratings,* Ph.D. Dissertation, School of Electrical Engineering, Cornell University, Ithaca, N.Y., August 1998.

10. C. E. Saavedra, W. Wright, K. Y. Hur, and R. C. Compton, "A Millimeter-Wave Quasi-Optical Amplifier Array using Inclined-Plane Horn Antennas," *IEEE Microwave and Guided Wave Lett.*, Vol. 8, No. 2, pp. 81-83, Feb. 1998.

11. N. J. Kolias and R. C. Compton "A Microstrip based Quasi-Optical Polarization Rotator Array," *IEEE MTT-S Digest,* pp. 773-776, 1995.

12. P. F. Goldsmith, "Quasi-Optical Techniques," *Proc. IEEE*, Vol. 80, No. 11, pp. 1729-1747, Nov. 1992.

13. HP 8510C Newtork Analyzer Operating and Programming Manual, Ed. No. 1, Hewlett Packard Company, June 1991.

14. S. J. Wilson, and M. C. Hutley, "The Optical Properties of 'Moth-Eye' Antireflection Surfaces," *Optica Acta,* Vol. 29, No. 7, pp. 993-1009, 1982.

15. J. Y. L. Ma, and L. C. Robinson, "Night Moth Eye Window for the Millimetre and Sub-Millimetre Wave Region," *Optica Acta* Vol. 30, No. 12, pp. 1685-1695, 1983.